Energy, Environment and Storage

Journal Homepage: www.enenstrg.com

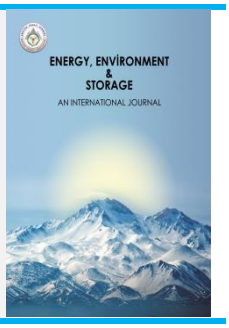

CFD MODELLING OF VOLTACAR ELECTRIC VEHICLE BODY FOR THE MOST EFFICIENT DRIVING CONDITIONS

Yakup Ogun SUZEN[1,4,5*], Emre OZDOGAN[2,4,5], Ibrahim SAN [3,4], Batuhan GURBUZ[2,4] Mehmet KACAR[3,4] Nesrin DEMİR[2,4,5] and Mehmet Fatih KAYA[*,2,4,5,6]

[1]*Department of Mechanical Engineering, Faculty of Engineering, Erciyes University, 38039, Kayseri, Turkey*

[2]*Department of Energy Systems Engineering, Faculty of Engineering, Erciyes University, 38039, Kayseri, Turkey*

[3]*Department of Mechatronic Engineering, Faculty of Engineering, Erciyes University, 38039, Kayseri, Turkey*

[4]*Erciyes University VoltaCAR Electromobile & Hydromobile Team, 38039, Kayseri, Turkey*

[5]*Erciyes University H2FC Hydrogen Energy Research Group, 38039, Kayseri, Turkey*

[6]*BATARYASAN Enerji ve San.Tic. Ltd.Şti, Yıldırım Beyazıt Mah., Aşık Veysel Bul., ERÜ TGB İdare ve Kuluçka 4, No: 67/3/11, Melikgazi, Kayseri, Turkey*

kayamehmetfatih@erciyes.edu.tr; ORCID: 0000-0002-2444-0583

ABSTRACT: In recent years, fossil fuels prices, greenhouse gas emissions, and need for sustainable energy sources have been increasing day by day. Thus, electric vehicles are seen as a promising candidate in the market due to their low-costs and cleaner fuel options such as electricity, hydrogen etc. Moreover, aerodynamics is one of the most important criteria to consider while designing an automobile for the most efficient driving conditions. For this reason, vehicle developers are studying to reduce drag resistance of the body to improve driving efficiency. On the other hand, Computational Fluid Dynamics (CFD) is one of the main tools for the automotive industry to obtain low-cost results before prototyping of any product. In this study, the aerodynamic characteristics of VoltaCAR electric vehicle is numerically investigated to obtain the best driving velocity. This car participates the TUBITAK-Electromobile car competition every year to achieve low fuel consumption for one hour driving. Thus, it is aimed that to minimize the resistance of the air hitting from the front, side, and roof of the vehicle. In the numerical model, polyhedral mesh structure is preferred to obtain faster convergence with fewer iterations, and shorter computation time is obtained compared to the tetrahedral mesh method. The aerodynamic drag coefficient (C_d) of the car model was calculated as approximately 0.17 at 22.22 and 27.78 m/s. The optimum velocity values were selected as 22.22 and 27.78 m/s by means of their lower C_d.

Keywords: Aerodynamics, Fuel-Efficiency, Drag Coefficient, Computational Fluid Dynamics, Electromobile, Polyhedral Mesh

Article History: Received:05.11.21; Revised: 15.11.2021; Accepted:26.11.2021; Availableonline: 26.11.2021
Doi: https://doi.org/ 10.52924/DGHR8227

1. INTRODUCTION

Energy consumption in developed and developing countries continues to increase day by day. Thus, energy demand will reach unsustainable levels in the future [1]. Today, the automotive industry is faced with challenges such as reducing emissions of exhaust gases into the atmosphere, increasing safe driving, and reducing the use of fossil-based fuels required for energy production. Therefore, use of hybrid and electric vehicles, biofueled cars and reducing engine sizes are very important for the sustainable transportation [2]. The development of electric cars has increased in response to the reality that future oil sources will be depleted. Since the last decade, electric vehicles have attracted a lot of attention as one of the potential solutions to reduce greenhouse gas emissions. About half of the total fuel energy is lost to come through the aerodynamic forces [3]. In a medium-sized car, the total resistance at 100 km/h is over 65% due to aerodynamics forces [4]. For this reason, vehicle developers are researching to reduce drag resistance. It also improves passenger comfort by providing ventilation, air conditioning, reducing mud formation on the vehicle, and reducing noise levels [5]. The aerodynamic development of the vehicle history has been gathered under two main headings. Firstly, it is focused on the wind that is hitting from the front of the vehicle (projectile area) at high speeds. Secondly, it is aimed to reduce the accumulation of mud or dirt on the windows and lights of the vehicles by arranging them according to the wing designs of the aircraft with an aerodynamic body [6]. CFD is a beneficial tools of fluid mechanics that uses numerical methods and algorithms to

solve and analyze problems involving fluid flows. CFD is one of the vital processes for the automotive industry [7, 8]. Thus, it is important for the efficient driving conditions for the electric cars as well. In the future, internal combustion engines will be replaced by electric vehicles, fuel cell vehicles, and hybrid vehicles. Limited driving range is one of the challenge due to battery developments of electrical vehicles [9, 10]. In Turkey, there are few competitions organized by TEKNOFEST and TUBITAK Efficiency Challenge is a college-level student design competition in which students from colleges around the country to design and compete with racetracks each year. In this study, CFD analysis of the vehicle is conducted for a full-scale car model to obtain most efficient numerical outputs for the low fuel consumption driving. The purpose of this study is to produce low C_d car and optimize the car velocity range during the one hour driving time.

2. MODEL DEFINITION AND NUMERICAL SOLUTION METHOD

2.1 Physical Model

Geometry of the model car was created with SolidWorks design software. Rendering of the model was performed in SolidWorks Visualize tool. In the design process, it is aimed to obtain a low C_d, so that the dimensions are suitable to the rules and there are no sharp edges on the vehicle body [11]. Figure 1 shows the side view and the isometric view of the vehicle model.

(a)

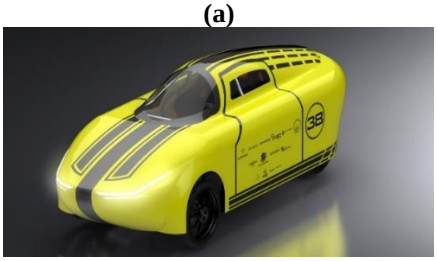

(b)

Figure 1. (a) Side view and **(b)** Isometric view of car model.

In Figure 2 the flow domain and boundary conditions can be seen.

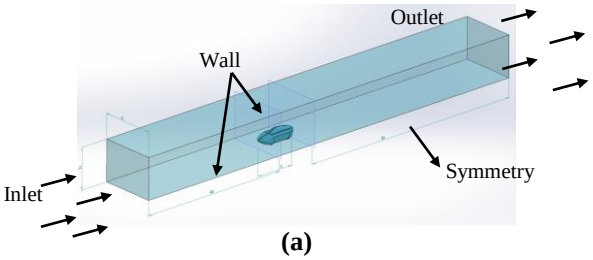

(a)

Figure 2. (a) Flow domain design and boundary regions.

As given in Figure 2 the flow domain was created around the car in the SpaceClaim to perform the analysis. Length of the vehicle is x, then the distance from starting of the virtual box to the front end of the car is 5x whereas from the rear end of the car to the end of the virtual box is 10x [12, 13].

2.2 Mesh Generation

In Figure 3, the mesh structures of the model which is generated by ANSYS Fluent can be seen. Polyhedral meshes are preferred due to their advantages such as faster convergence with fewer iterations, the accuracy of wall shear stresses, and shorter computation time compared to the tetrahedral mesh method.

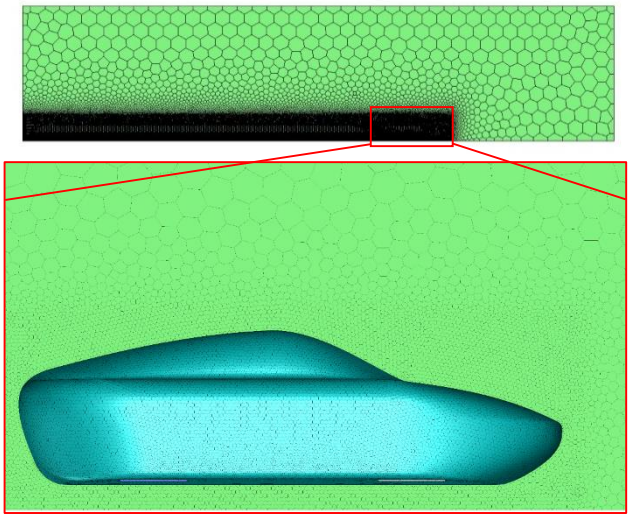

(a)

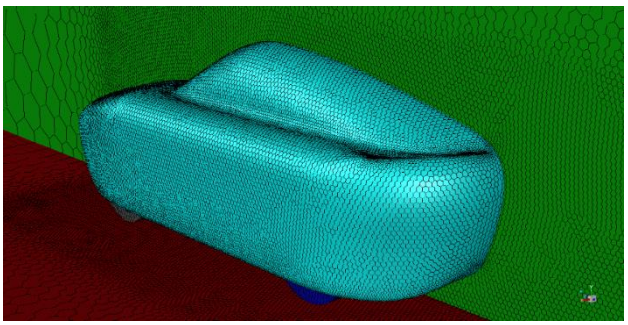

(b)

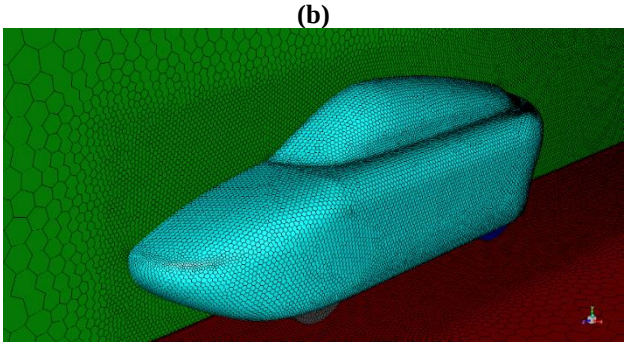

(c)

Figure 3. (a) Detailed view (**b)** Rear Isometric view (**c)** Front Isometric view of polyhedral meshing

The inlet flow is assumed as isothermal and incompressible, and the velocity of the air is set to 27.78,

22.22, and 16.67 m/s, respectively. The velocity values for the vehicle aerodynamics were performed according to the competition time as given in the rules completing for one hour. Therefore, according to racing track length, velocity was selected as the range of 16.67, 22.22 and 27.78 m/s. Also, the car body, ground plane, and wheels are defined as no-slip wall. At the outlet, the boundary condition is selected as a pressure outlet with a gauge pressure of 0 Pa [14-16]. There are approximately 2984497 polyhedral cell and 4459322 nodes in the model. In Figure 4, inlet and outlet region of the mesh structure can be seen.

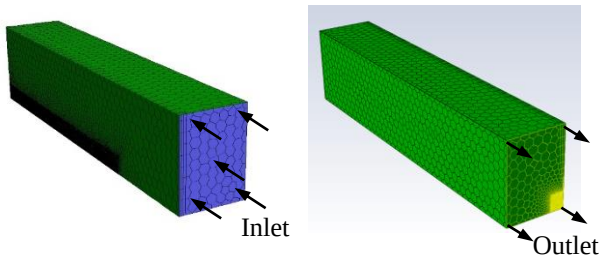

Figure 4. (a) Inlet area, **(b)** outlet area for meshing

2.3. Mathematical Model

Laminar and turbulent flow are the two different forms of the flow. Laminar flow is defined as fluid particles are moving parallel to each other at a constant speed and without or smaller mixing condition with each other. On the other hand, turbulent flow is a kind of fluid motion that is described by chaotic changes in flow velocity and pressure [17-19].

Thus, the flow around the vehicle body can be defined by Navier-Stokes equation as given Eq.1 [20]:

$$\boldsymbol{\rho\left(\frac{\partial u_i}{\partial t}+u_j\frac{\partial u_i}{\partial x_j}\right)=-\frac{\partial P}{\partial x_i}+\mu\frac{\partial^2 u_i}{\partial x_j\partial x_j}+f_i} \quad (1)$$

Where u represents the velocity, t is the time, x is the position, P is the pressure, and ρ is density in kg/m^3. In the numerical model, k – ε turbulent model is used and transport equations for standard k – ε turbulent model can be written as Eq. 2:

$$\frac{\partial}{\partial t}(\rho k)+\frac{\partial}{\partial x_i}(\rho k u_i)=\frac{\partial}{\partial x_j}\left[\left(\mu+\frac{\mu_t}{\sigma_k}\right)\frac{\partial k}{\partial x_j}\right]+G_b+G_k-\rho\varepsilon-Y_m+S_k \quad (2)$$

In these equations, G_b is the generation of turbulence kinetic energy due to buoyancy, G_k represent the generation of turbulence kinetic energy due to the mean velocity gradients, Y_m describes the contribution of the fluctuating dilatation incompressible turbulence to the overall dissipation rate. C_{1e}, C_{2e} and C_{3e} are constants. σ_k and σ_ε are the turbulent Prandtl numbers for k and ε, respectively. S_k and S_e are user-defined source terms. C_f is the skin-friction coefficient.

To model dissipation (ε) Eq.3 can be used:

$$\frac{\partial}{\partial t}(\rho\varepsilon)+\frac{\partial}{\partial x_i}(\rho\varepsilon u_i)=\frac{\partial}{\partial x_j}\left[\left(\mu+\frac{\mu_t}{\sigma_\varepsilon}\right)\frac{\partial\varepsilon}{\partial x_j}\right]+C_{1\varepsilon}\frac{\varepsilon}{k}(G_k+C_{3\varepsilon}G_b)-C_{2\varepsilon}\rho\frac{\varepsilon^2}{k}+S_\varepsilon \quad (3)$$

To model shear stress (τ_w) on the wall Eq.4 can be used [21]:

$$\tau_w=\frac{C_f\rho U_{freestream}^2}{2} \quad (4)$$

Conservation of mass, momentum, and energy are fundamental equations for CFD calculations [22]. Eq.5 can be used to calculate Reynolds number as below:

$$\boldsymbol{Re=\frac{\rho VL}{\mu}} \quad (5)$$

In this equation, V represents velocity of the fluid in m/s, μ describes dynamic coefficient of viscosity in N.s/m^2, and L is the characteristic length in m. Reynolds number is a dimensionless number that can be used to describe the flow of fluid[23].

Aerodynamic drag force (F_d) causes more resistance force in passenger automobiles at higher speeds. It is a resistive force that affects the performance of a vehicle. Also, this component of resistance might become overpowering at high speeds [24]. Thus, vehicle developers have challenge to reduce drag resistance. In Figure 5, F_d and lift force (F_L) regions can be seen.

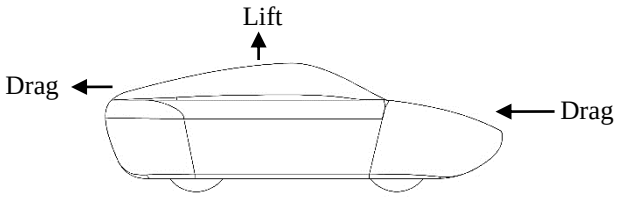

Figure 5. F_d and F_L on the vehicle body.

F_d is known as the force parallel to the flow direction. The drag coefficient (C_d), which is a dimensionless number, is given as Eq.6 below:

$$\boldsymbol{C_d=\frac{2F_d}{\rho V^2 A}} \quad (6)$$

Where F_d is drag force in N, ρ is density in kg/m^3, V is velocity in m/s, and A is the refence area in m^2. Reference area of the model can be seen as given in Figure 6.

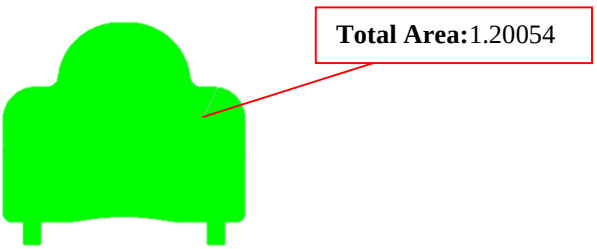

Figure 6. Reference area

The C_d of the vehicles are approximately 1.0 for large semi-trailers, 0.4 for minivans, and 0.3 for passenger cars [25].

The component of the aerodynamic force perpendicular to the direction of flow is defined as the F_L. F_L is very important to ensure the controllability of the vehicles and as the speed increases. The lift coefficient (C_L) is a dimensionless coefficient that relates the lift created by a lifting body to the fluid density over the body, the fluid velocity, and a reference area can be calculated by Equation (7).

$$C_L = \frac{F_l}{\frac{1}{2}\rho V^2 A} \quad (7)$$

In Table 1, the solution parameters for the Ansys model can be seen.

Table 1. Fluent solver parameters

Solver		Fluent		
Formulation		Implicit		
Time		Steady		
Temperature (K)		288.16		
Velocity (m/s)		16.67	22.22	27.78
Area (m^2)		0.60027 (Symmetry)		
Velocity Formulation		Absolute		
Gauge Pressure (Pascal)		0		
Turbulence Models		SST-k- ε Realizable-Enhanced Wall Treatment		
		SST–k-ω		
Scaled Residuals		10^{-4}		
Fluid Properties	**Fluid Type**	Air		
	Density	ρ = 1.225 (kg/m^3)		
	Viscosity (kg/m-s)	1.7894e-05		

3. RESULTS AND DISCUSSION

CFD-Post software is used to determine streamlines, pressure, velocity distributions, velocity vectors, C_d, and pressure results. In Figure 7, streamlines and velocity display can be seen around the vehicle body.

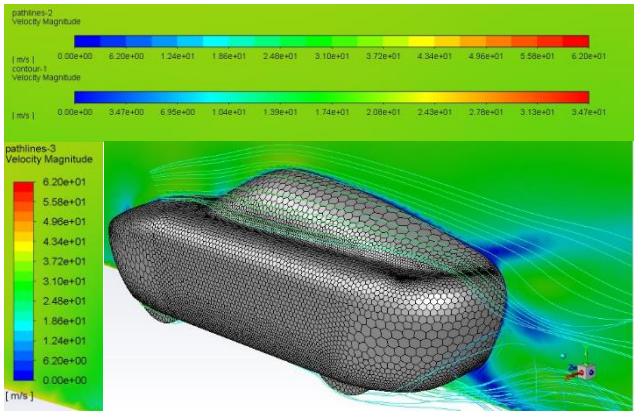

Figure 7. Streamlines and velocity display

To understand the flow around the model, a flow visualization test was performed in the Ansys Post-processing .The flow analysis on the vehicle is performed on three different inlet velocity such as 16.67, 22.22, 27.78 m/s to get the results for the C_d, and C_L.

For 16.67 m/s inlet velocity, it has been observed that the F_d of the vehicle decreases with the C_d and C_L, respectively. C_d, and C_L are became stable after 100 iterations and the residual graph is converged. C_d and C_L are calculated as 0.1818, and 0.09531, respectively. In Figure 8, at 16.67 m/s, pressure, turbulent kinetic energy, velocity magnitude, and wall shear stress can be seen.

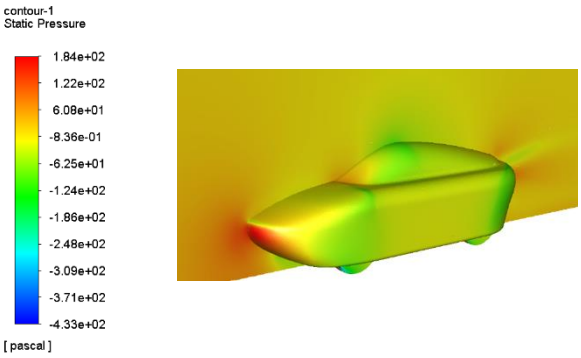

(a)

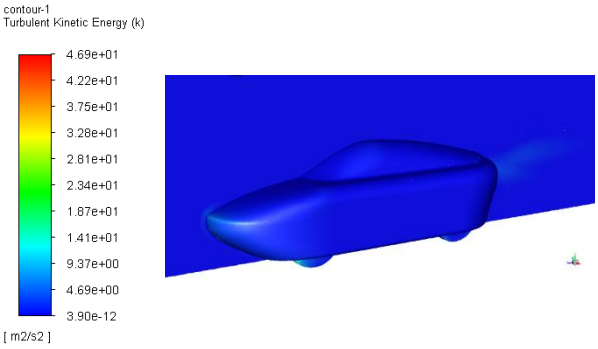

(b)

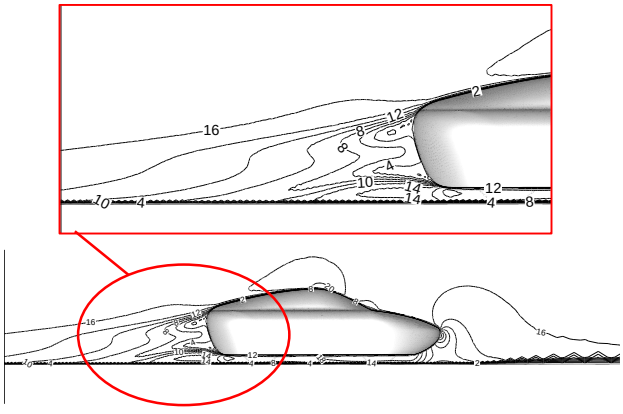

(c)

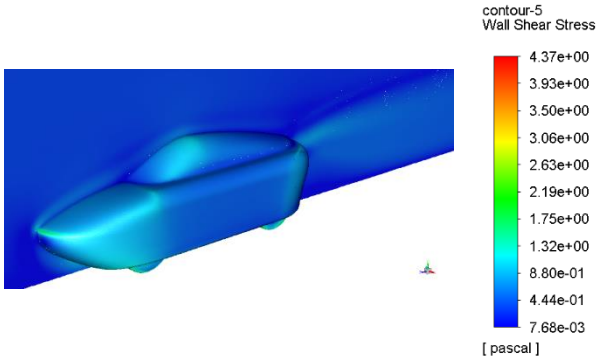

(d)

Figure 8. (a) Pressure, **(b)** Turbulent Kinetic Energy , **(c)** Velocity Magnitude, and **(d)** Wall Shear Stress figures at 16.67 m/s

Figure 8. (a) shows the pressure contours over the vehicle body and the maximum pressure occurs front surface of the car. The minimum pressure value occurs in the separated flow region. This is due to the fluid's velocity being close to zero in these regions. Pressure values at low speeds, relatively lower than at higher speeds. According to the pressure distribution on the symmetric surface, the maximum and minimum pressures are calculated as 153 Pa and -93 Pa, respectively. Figure 8. (b) shows the contour of turbulence kinetic energy on the symmetry plane. Figure 8. (c) represent the velocity streamlines in the symmetry plane. Figure 8. (d) shows the wall shear stress distribution in the body. The stress values are small which is around 0.2-2 Pa in the vehicle body. Separated airflows may occur in the shear stress which are close to 0 point like wheel and underbody of the vehicle. The vortex under the vehicle not only increases the aerodynamic drag but also increases the pressure drag by changing the flow area behind the vehicle.[26]

C_d, and C_L are became stable after 125 iterations and the residual graph is converged. C_d and C_L are calculated as 0.1801, and 0.0939, respectively. These C_L and C_d values show better aerodynamics characteristics when the car move faster. In Figure 9 shows the pressure, velocity, turbulent kinetic energy and wall shear stress distrubution of the vehicle body at 22.22 m/s.

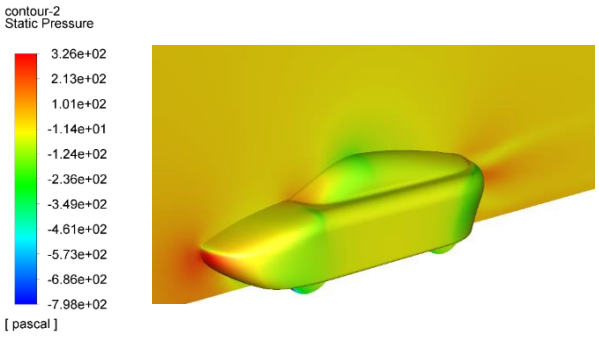

(a)

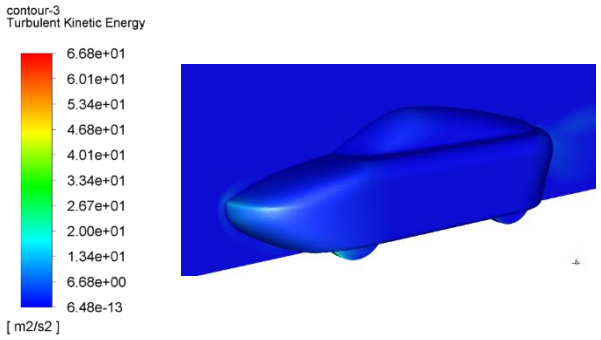

(b)

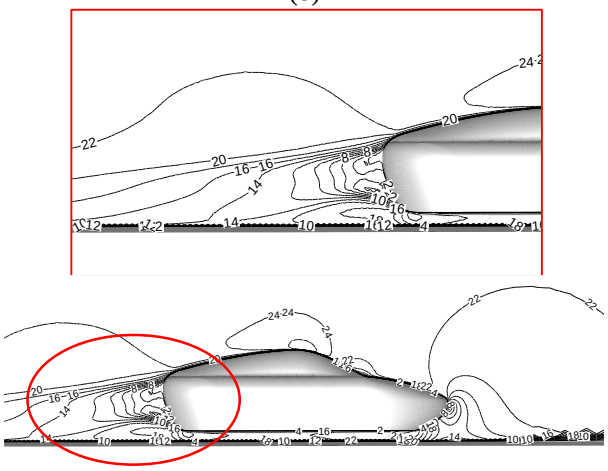

(c)

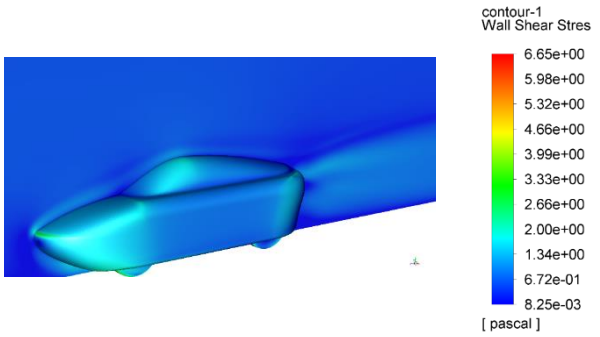

(d)

Figure 9. (a) Pressure, **(b)** Turbulent Kinetic Energy , **(c)** Velocity Magnitude, and **(d)** Wall Shear Stress figures at 22.22 m/s

Figure 9. (a), and (c) shows the pressure contour and velocity magnitude all over the vehicle body. According to the pressure distribution on the symmetric surface, the maximum and minimum pressures are calculated as 270 Pa and -180 Pa, respectively. As shown in Figure 9. (a) pressure values are increased by velocity increment. The maximum value of turbulence kinetic energy was found in the vehicle's rear section. As seen in the Figure 9. (d) wall shear stresses increase with respect to speed especially on the front panel and rear side of the car body.

The C_d and C_L are calculated as 0.1788 and 0.0926 respectively. C_L is decreased from 0.0939 to 0.0926. In Figure 10 shows the static pressure, turbulent kinetic energy, velocity and wall shear stress can be seen. As shown in Figure 9. (a) pressure values increase due to velocity increment. The maximum and minimum pressures

are calculated as 300 Pa and -240 Pa, respectively, As seen in the Figure 9, wall shear stresses on the rear side of the vehicle is close to 0 which may occur separated airflows with respect to the turbulence. The stress values are small which is around 1.2- 4 Pa in the vehicle body. The results of the C_d and C_L at different speeds and turbulence models can be seen in Table 2.

Table 2: C_d and C_L Results in turbulence model SST-k- ε Realizable – Enchanced Wall Treatment and SST-k-ω

RESULTS		Velocity (m/s)		
		16.67	**22.22**	**27.78**
SST-k- ε Realizable- Enhanced Wall Treatment	**C_d**	0.1833	0.1823	0.1636
	C_L	0.1684	0.1674	0.1140
SST–k-ω	**C_d**	0.1818	0.1801	0.1788
	C_L	0.09531	0.0939	0.0926

As seen in the Table, in the higher speed, F_d increases. This increment occurs at the front of the vehicle. As can be seen from the table, C_d in terms of fuel consumption at 22.22 - 27.78 m/s shows more efficient driving. On the other hand, the air inlet from under the vehicle exerts pressure to lift the vehicle up, so in case of any bending, the vehicle may be easily skidded, and it may cause rolling over during the road driving. For this reason, automotive developers are tried to increase the downforce by giving curvature to the infrastructure of the cars. As given in Table 2, the C_L value for this vehicle is calculated as between 0.00201 and 0.00719. The results were compared with another turbulence model, SST k-ω, and it was found that there is no any significant difference between the results**.**

Figure 10 (a), and (c) shows the pressure contour and velocity magnitude all over the vehicle body. According to the pressure distribution on the symmetric surface, the maximum and minimum pressures are calculated as 270 Pa and -180 Pa, respectively. As shown in Figure 10 (a) pressure values increase due to velocity increment. The maximum value of turbulence kinetic energy was found in the vehicle's rear section. As seen in the Figure 10 (d) wall shear stresses increase with respect to speed especially on the front panel and rear side. In higher speed values, F_d value is increased. The aerodynamic F_d on the vehicle are dominant at 22.22 -27.78 m/s speeds, which is an important place in flow analysis. Therefore, the F_d and aerodynamic frictions in the vehicle is important parameter for fuel consumption which is desired to reduce pressure on the front vehicle. F_d on the car is around 40-60 N at 22.22 and 27.78 m/s. It has been observed that due to the turbulence regions formed at high speeds the graph is more difficult to converge than at low speed.

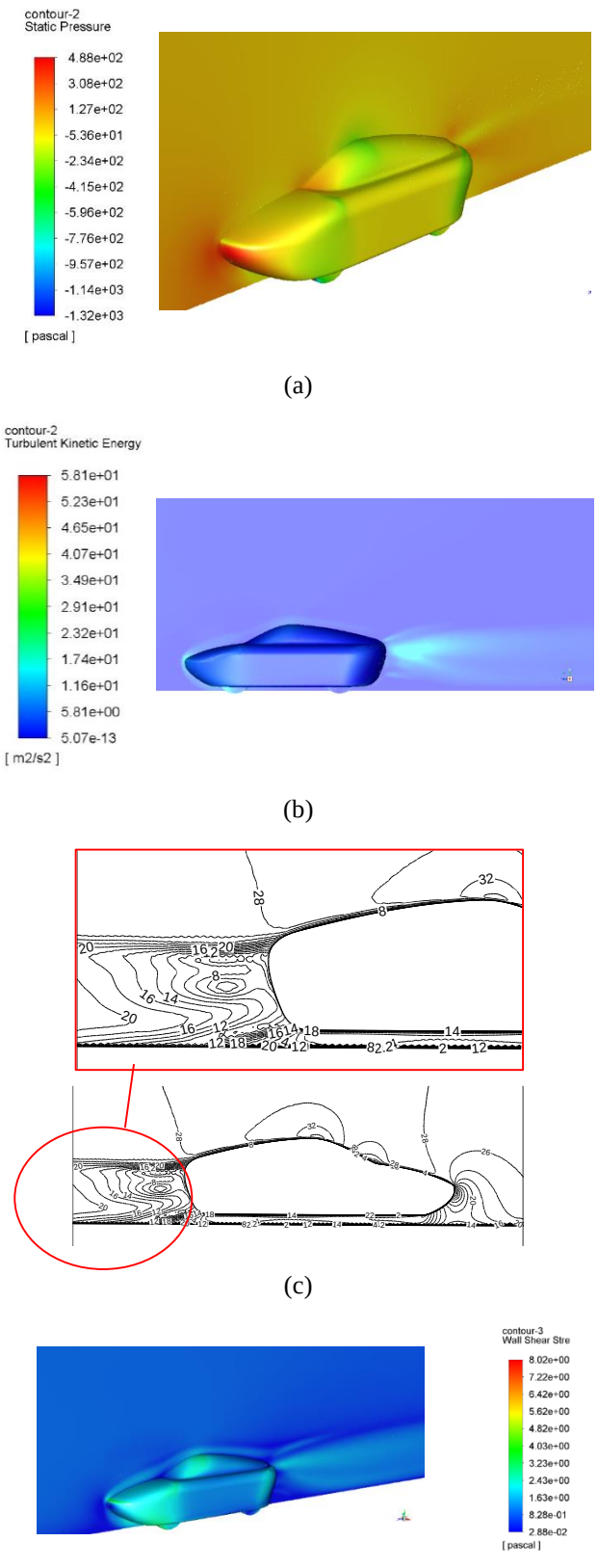

Figure 10. (a) Pressure, **(b)** Turbulent Kinetic Energy , **(c)** Velocity Magnitude, and **(d)** Wall Shear Stress figures at 27.78 m/s

The C_d have closer results compared to the F_d. It can be also observed that the same situation caused by the turbulence zone is obtained in C_d results. When C_d value of the vehicle has increased, fuel consumption increases, also

performance losses occur. As a result, C_d is computed approximately 0.17 at 22.22 – 27.78 m/s. For this reason, the C_d has an important place for automotive industry.

4. CONCLUSION

The aerodynamic characteristics of the body shape of the VoltaCAR, which was produced to participate in the TUBITAK Efficiency Challenge race, is realized in 3D numerical model using ANSYS Fluent software. This vehicle design was conducted according to the race rules. For numerical modeling, the mesh method was preferred as polyhedral, thus shortening the solution time and faster converge for the solution. The static pressure is calculated approximately as 270 Pa on the front side of the vehicle and between 67-120Pa on the vehicle body at 22.22 m/s. Also, the static pressure which is on the front side of the vehicle has increased approximately 400Pa, and in the vehicle body, it is between 55 and 150 Pa at 27.78 m/s. The pressure created by the air affects the front of the vehicle. It is distributed to the lower and upper sides along with the slope in the vehicle design, thus allowing the wind to flow more smoothly, thereby reducing the pressure. Depend on the speed, there is 50% much more static pressure is obtained on the front of the vehicle, but this increase is lower than the vehicle body. Thanks to these results, the pressure increase of the vehicle body is minimized. On the other hand, the Also, the aerodynamic C_d of the car model is found approximately 0.11 at 22.22 and 27.78 m/s. As a conclusion when increasing the speed, the Cd decreases, but the Fd and pressures at the side of the vehicle increase. Passenger vehicles have an average C_d of 0.25, the C_d computed for this vehicle design is much lower depending on its speed. As a result, the most efficient fuel consumption range for this vehicle was determined between 22.22 and 27.78 m/s. For the race conditions, these parameters can be further improved by optimizing critical points of the flow with aerodynamics experimental studies.

Acknowledgements

Authors would like to thank TÜBİTAK Efficiency Challenge Organization Committee and all Enerjist-VoltaCAR Electric and Hydrogen Fuel Cell car project team members for their great effort on the car design and production successfully.

REFERENCES

[1] Michaelides EES. (2012). Alternative energy sources: Springer Science & Business Media..
[2] Davila A, Aramburu E, Freixas A. (2013). Making the best out of aerodynamics: Platoons. SAE Technical Paper.
[3] Hassan SR, Islam T, Ali M, Islam MQ. (2014). Numerical study on aerodynamic drag reduction of racing cars. Procedia Engineering. 90:308-13.
[4] Wood R. (2015). Reynolds number impact on commercial vehicle aerodynamics and performance. SAE International Journal of Commercial Vehicles.8:590-667.
[5] Sivaraj G, Parammasivam K, Suganya G. (2018). Reduction of aerodynamic drag force for reducing fuel consumption in road vehicle using basebleed. Journal of Applied Fluid Mechanics.11:1489-95.
[6] Sivaraj G, Parammasivam K, Prasath M, Vadivelu P, Lakshmanan D. (2021). Flow analysis of rear end body shape of the vehicle for better aerodynamic performance. Materials Today: Proceedings.
[7] Pal S, Kabir S, Talukder M. (2015). Aerodynamic analysis of a concept car model. Proceedings of the third ICMERE.26-9.
[8] Chandra S, Lee A, Gorrell S, Jensen CG. (2011). CFD analysis of pace formula-1 car. Computer-Aided Design & Applications, PACE (1):1-14.
[9] Nalanagula S, Varadharajan G. (2016). Aerodynamics drag reductions methodology for the commercial vehicles using computational fluid dynamics. SAE Technical Paper.
[10] Huluka AW, Kim C-H. (2021). A Numerical Analysis on Ducted Ahmed Model as a New Approach to Improve Aerodynamic Performance of Electric Vehicle. International Journal of Automotive Technology.22:291-9.
[11] Lanfrit M. (2005). Best practice guidelines for handling Automotive External Aerodynamics with FLUENT. Version.
[12] Kaluva ST, Pathak A, Ongel A. (2020). Aerodynamic drag analysis of autonomous electric vehicle platoons. Energies.13:4028.
[13] Watanabe K, Matsuno K. (2009). Moving computational domain method and its application to flow around a high-speed car passing through a hairpin curve. Journal of computational Science and Technology. 3:449-59.
[14] Spiegel M, Redel T, Zhang YJ, Struffert T, Hornegger J, Grossman RG, et al. (2011). Tetrahedral vs. polyhedral mesh size evaluation on flow velocity and wall shear stress for cerebral hemodynamic simulation. Computer methods in biomechanics and biomedical engineering. 14:9-22.
[15] Balafas G. (2014). Polyhedral mesh generation for CFD-analysis of complex structures. Diplomityö Münchenin teknillinen yliopisto.
[16] Kleber A. (2001). Simulation of airflow around an Opel Astra vehicle with Fluent. Journal Article, International Technical Development Center Adam Opel AG.
[17] Hoffman J, Johnson C. (2007). Laminar and Turbulent Flow. Computational Turbulent Incompressible Flow: Applied Mathematics: Body and Soul 4. 51-5.
[18] Vasamsetti S. Streamlining and Aerodynamic Performance Add-on Devices of Sports Cars.
[19] Batchelor CK, Batchelor G. (2000). An introduction to fluid dynamics: Cambridge university press.
[20] Hetawal S, Gophane M, Ajay B, Mukkamala Y. (2014). Aerodynamic study of formula SAE car. Procedia Engineering.97:1198-207.
[21] Thabet S, Thabit TH. (2018). CFD simulation of the air flow around a car model (Ahmed body). International Journal of Scientific and Research Publications. 8:517-25.
[22] Damjanović D, Kozak D, Živić M, Ivandić Ž, Baškarić T. (2011). CFD analysis of concept car in order to improve aerodynamics. Járműipari innováció. 1:108-15.
[23] Shi X, Sun DJ, Zhang Y, Xiong J, Zhao Z. (2020). Modeling emission flow pattern of a single cruising vehicle on urban streets with CFD simulation and wind tunnel validation. International Journal of Environmental Research and Public Health;17:4557.
[24] Mannering FL, Washburn SS. (2020). Principles of highway engineering and traffic analysis: John Wiley & Sons.
[25] Sofian M, Nurhayati R, Rexca A, Syariful SS, Aslam A. (2014). An evaluation of drag coefficient of wind turbine system installed on moving car. Applied Mechanics and Materials: Trans Tech Publ; p. 689-93.
[26] Yuan Z, Wang Y. (2017). Effect of underbody structure on aerodynamic drag and optimization. Journal of Measurements in Engineering. 5:194-204.